Journal of Colloid and Interface Science 467 (2016) 115–120

Contents lists available at ScienceDirect

Journal of Colloid and Interface Science

journal homepage: www.elsevier.com/locate/jcis

Single-crystal Au microflakes modulated by amino acids and their sensing and catalytic properties

Mingjie Li, Xiaochen Wu, Jiyu Zhou, Qingshan Kong, Chaoxu Li *

CAS Key Laboratory of Bio-Based Materials, Qingdao Institute of Bioenergy and Bioprocess Technology, Chinese Academy of Sciences, Songling Road 189, Qingdao 266101, PR China

GRAPHICAL ABSTRACT

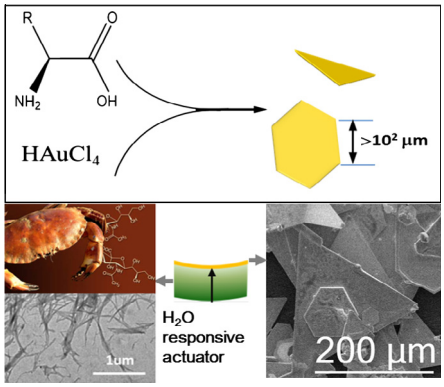

ARTICLE INFO

Article history:
Received 1 December 2015
Revised 1 January 2016
Accepted 4 January 2016
Available online 5 January 2016

Keywords:
Single-crystal Au microflakes
Chitin nanofibrils
Humidity response
Biosensor

ABSTRACT

Single-crystal Au microflakes with the planar area over 10^3 μm^2 (i.e. being accessible to the human eye resolution) were synthesized in an environment-friendly route by directing two-dimensional growth of Au nanocrystals into macroscopic scales with amino acids as both reducing agents and capping agents. Side groups of amino acids were found to be a determinant parameter to tune the dimension and size of Au single crystals. The successful synthesis of Au microflakes provides an unprecedented opportunity to bridge nanotechnology and macroscopic devices, and hereby to start a new scenario of exploring their unique properties and applications in optoelectronic devices and bio-sensing fields across multiple length scales. For example, Au microflakes respond to air humidity upon depositing on films of chitin nanofibrils, and sense various physiological molecules as electrode materials of biosensors.

1. Introduction

Owing to outstanding combination of unique atomic structure, stability and quantum size effect, Au nanocrystals have been revealed with fascinating structure-/environment-dependent properties and hereby promised diverse applications in catalysis, electronics, photonics, plasmonics, and biomedicine [1,2]. Among various shapes of Au nanocrystals, the discovery of exceptional anisotropic features and atomically flat surfaces in two-dimensional single-crystal Au crystals (2DAC) triggered particular interests in optoelectronic devices and bio-sensing fields based on their unique properties (e.g. surface plasmon resonances, conductivity, catalytic efficiency and affinity with biomolecules) [3]. Developing novel approaches to enable full shape/size control of

* Corresponding author.
E-mail address: licx@qibebt.ac.cn (C. Li).

http://dx.doi.org/10.1016/j.jcis.2016.01.004
0021-9797/

2DAC has become one of the most attractive and active subjects under investigation [1]. For instance, besides regular shapes (triangle, hexagon and truncated hexagon), belt-like and shield-like geometries have been produced by finely tuning free energies of different crystallographic facets of Au nanocrystals in a "kinetically controlled" synthesis pathway [3]. The thickness within a broad range of 5–150 nm was achieved by carefully selecting soft/interfacial templates and capping agents. Notwithstanding these encouraging findings, however, limited lateral dimension still severely hinders the transference of unique 2D effect of 2DAC across multiple length scales demanded in practical applications [4,5], e.g. precisely positioning tips of 2DAC for nano-focus effect in gas sensing devices [6].

Despite repeated endeavour on pushing up the lateral dimension of 2DAC, it remains highly challenging to synthesize single-crystal Au microflakes with the planar area over 10^3 μm^2 (i.e. being accessible to the human eye resolution). According to the typical nucleation-and-growth mechanism of 2DAC [7], larger lateral sizes could be achieved through lessening their nuclei and slowing down the growth process, which, however, were less than 1 μm in most cases (i.e. nanoplates). On the other hand, a lateral size over 1 μm could be produced in principle through a mechanism of reorganization and interconnection of Au nanocrystals, where small nanoplates connect together along their lateral planes with higher free energy [3]. This process has been noted at interfaces of solid–liquid [8] and liquid–liquid [9], and within self-assemble lamellar structures in the presence of surfactants [10] and/or block copolymers [11].

In analogue to the bio-evolution which creates complex and "life-like" organic materials scaled in 10^0–10^9 nm in green and benign chemistry, bio-mimetic synthesis processes have also shown their potential to yield series of inorganic materials with hard-to-reach structures and properties with the assistance of biological molecules [12]. For example, a lateral dimension up to 20 μm was shown in bio-synthesis of 2DAC where proteins [13] and polysaccharides [14] were employed to direct the 2D growth of Au plates. We discovered the possibility of synthesizing single-crystal Au microflakes with the help of protein assemblies [5], despite poor control on their size, complicated synthesis procedures and sensitivity to reaction parameters.

As pioneering organic molecules in universe and basic building units of proteins, amino acids have shown their superiority in sophisticated bio-mineralization in living systems. By tuning their side groups, amino acids are expected as all-round molecules in bio-mimetic synthesis of diverse nanomaterials. Actually, spherical Au nanocrystals have been successfully synthesized by using amino acids both as reducing agent and capping agent [15–17]. 2DAC with the lateral size <1 μm was also synthesized by certain amino acids (e.g. aspartate [18] and tryptophan [17]), yet with the help of synthetic capping agents [17] and at high temperatures [19]. In spite of these inspiring studies, to the best of our knowledge, no attempt has been made to systematically investigate the correlation of side groups of amino acids and morphology control of Au crystals. Single-crystal Au microflakes have also not been synthesized with amino acids.

In this study we show that side groups of amino acids could be a determinant parameter to tune the dimension and size of Au single crystals. Not only 2DAC could be synthesized in a facile environment-friendly process, but also their lateral size could be extended to the human eye resolution. The successful synthesis of Au microflakes may provide an unprecedented opportunity to bridge nanotechnology and macroscopic devices, and hereby to start a new scenario of exploring their unique properties and applications in optoelectronic devices and bio-sensing fields across multiple length scales.

2. Experimental Section

2.1. Materials

Amino Acids (L-lysine, L-arginine, L-tryptophan, L-aspartic acid and L-glutamic acid) and tetrachloroauric acid ($HAuCl_4$, 48% Au basis) were purchased from Sigma and used without any further purification.

2.2. Preparation of 2D Au crystals

Calculated quantities of two solutions of $HAuCl_4$ (10 mM, pH 2) and amino acids (20 mM, pH 2) were added sequentially into Millipore water (pH 2) to achieve a homogenous mixture, in which the $HAuCl_4$ concentration was kept at 1.0 mM while the amino acid concentration was tuned at 0.5, 1.0, 2.0 or 5.0 mM. The reaction continued at 70 °C without stirring for different periods of time before quenching into ice–water. The final suspensions were centrifuged at 5000 rpm for 10 min. After several washing cycles with ethanol, the resultant products were maintained at 4 °C before characterization.

2.3. Preparation of chitin nanofibrils

Chitin nanofibrils were extracted from crab shell powder in a four-step protocol: (1) Crab shell powder was sequentially treated with 9% (v/v) HCl and 10 wt% NaOH solutions by vigorously stirring for 10 h and then centrifuged at 10,000 rpm for 15 min. (2) The precipitation was re-dispersed in 30 wt% NaOH by vigorously stirring for 1.5 h at 90 °C before washing with Millipore water to pH ~ 7. (3) The precipitation was suspended in water (pH 3.5, tuned with acetic acid). After magnetically stirred at 1300 rpm for 3 days and ultrasonically treated (300 W, 45 kHz) for 30 min, the resultant solution was dialyzed (cutoff: 6000 Da) with Millipore water. (4) The final solution of chitin nanofibrils was adjusted to pH ~ 3.5 and stored at 4 °C.

2.4. Preparation of chitin-Au bilayer films

The dispersion of chitin nanofibrils was vacuum-filtered with a Nylon filtration membrane (pore size of 0.2 μm, diameter of 47 mm) before filtering the suspension containing 2D Au crystals. The thicknesses of two layers were controlled by the volumes of the two dispersions. After finishing the filtration process, the film was air-dried for one week before further characterization.

2.5. Characterization

Scanning electron microscope (SEM) measurements were performed on Hitachi S-4800 operated at 10 kV. The specimens were mounted on SEM stubs with carbon conductive tabs, and then sputter-coated with a ~3 nm platinum layer. The Ultraviolet–visible (Uv–vis) spectrophotometric analysis was performed on DU800 Uv–vis spectrophotometer at ambient temperature. All the solutions were diluted to appropriate concentrations and scanned in 1 cm-path-length quarts cuvettes with the wavelength scan mode between 200 and 800 nm. The scan speed was 400 nm/min and the sample interval was 1.0 nm. Conductivity measurements were tested with Guangzhou Probes Tech RTS-8 Four Probes Detector. Electrochemical measurements were performed on an electrochemical analyzer (CHI 660E, CH instruments, Inc., Shanghai) with a three-electrode cell, in which an Ag/AgCl electrode was the reference electrode and platinum foil served as counter electrode. A modified glassy carbon electrode (GCE) was prepared by a simple casting procedure as the working electrode. 2D Au crystals were synthesized with amino acids and washed three times with

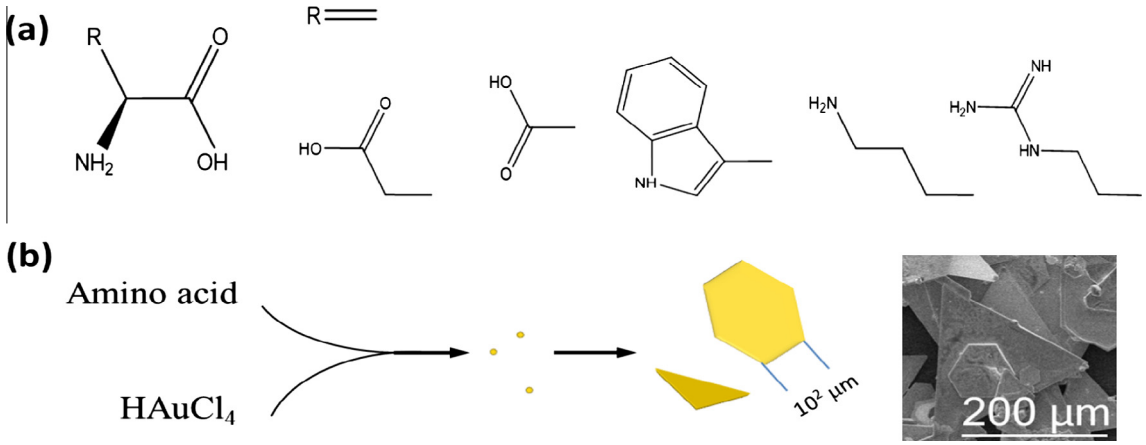

Fig. 1. (a) Chemical structures of amino acids used in this study. (b) Schematic illustration of synthetic routes of Au microflakes. The inset gives a typical SEM image of Au microflakes.

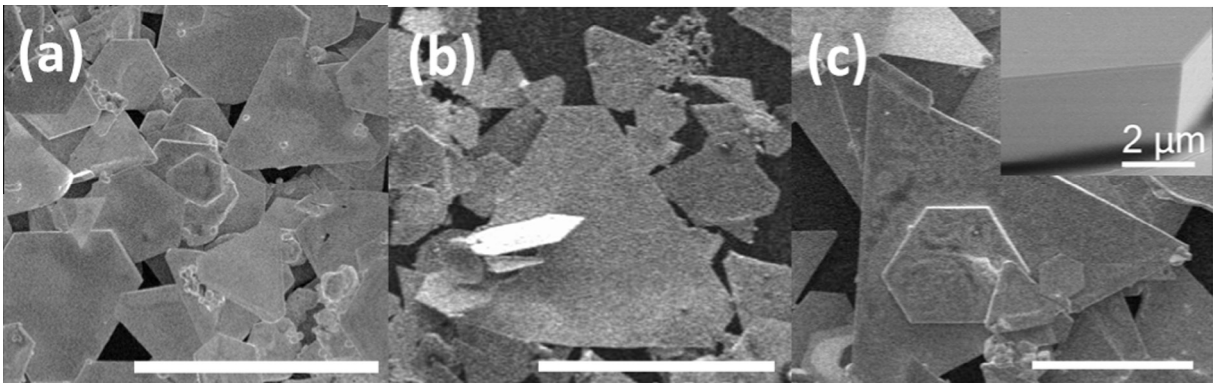

Fig. 2. SEM images of Au microflakes synthesized with (a) 2.0 mM L-tryptophan, (b) 1.0 mM L-glutamic acid and (c) 1.0 mM L-arginine. Experimental parameters: 1.0 mM tetrachloroaurate ions, 1.0 mM amino acid, 70 °C, pH 2, 50 h. The scale bars in figure (a–c) are 100 μm.

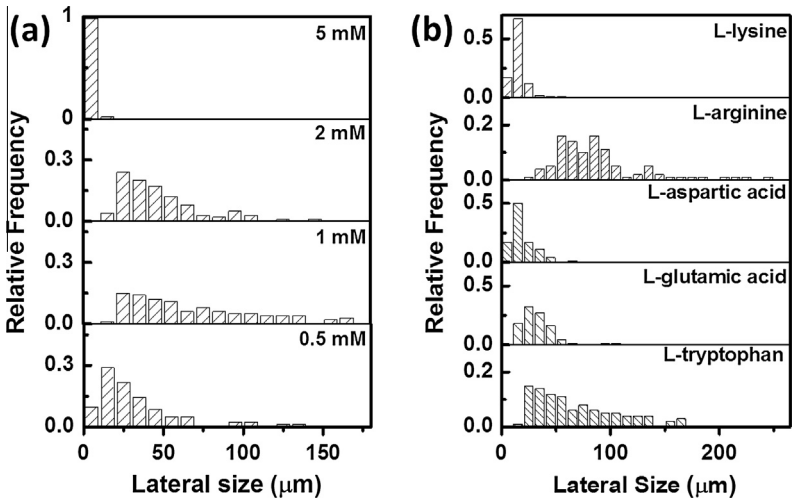

Fig. 3. Lateral size distribution of 2D Au nanocrystals synthesized (a) with L-tryptophan at different concentrations, and (b) with 1.0 mM amino acids with different side groups. Experimental parameters: 1.0 mM $HAuCl_4$, 1.0 mM amino acid, 70 °C, pH 2, 50 h.

ethanol. This suspension in ethanol was then casted on the surfaces of GCEs and air-dried for 8 h. The cyclic voltammetry (CV) and differential pulse stripping voltammetry (DPSV) were obtained in PBS buffer (0.2 M, pH 7.4 for CV and pH 6.0 for DPSV, and saturated N_2) with certain amount of H_2O_2, ascorbic acid (AA) and/or dopamine (DA) at a scanning rate of 50 mV/s.

3. Results and discussion

In order to investigate the effect of side groups of amino acids on morphologies of Au single crystals, five amino acids characteristic of indole group (L-tryptophan), carboxylic group (L-glutamic acid and L-aspartic acid), guanidino group (L-arginine) and amine

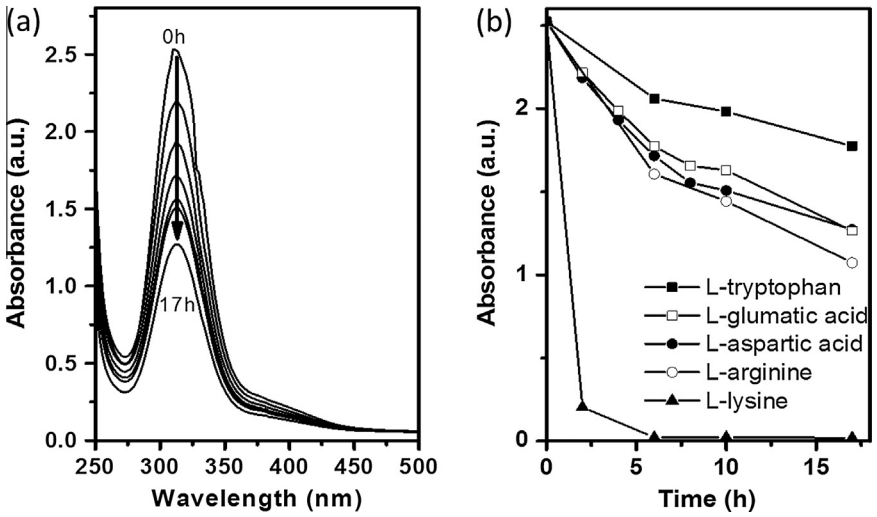

Fig. 4. (a) Time-resolved Uv–vis spectrophotometry of tetrachloroaurate ions reduced by 1.0 mM L-aspartic acid. (b) Variation of Uv–vis absorbance at 311 nm of tetrachloroaurate ions in the presence of different amino acids. Experimental parameters: 1.0 mM tetrachloroaurate ions, 1.0 mM amino acid, 70 °C, pH 2.

group (L-lysine) were examined (Fig. 1). In sharp contrast to spherical Au nanocrystals synthesized in most of previous studies [20,21], 2DAC with regular shapes (e.g. triangular, hexagonal and truncated triangular) were synthesized at pH 2, 70 °C and 1.0 mM $HAuCl_4$ (see Fig. 2), being independent of side groups of amino acids (Fig. S1). Furthermore, there exists an optimized concentration of amino acids within 0.5–2.0 mM to minimize the formation of Au spheres (see Fig. S1) and maximize the sizes of 2DAC up to Au microflakes (Figs. 3a and S2). In view of the structural feature of {1 1 1} crystal facets on both the top and bottom surfaces in most 2DAC, moderate reducing rates and strong capping effect (i.e. chemisorption selectivity to {1 1 1} crystal facets) are experimentally preferred to synthesize 2D Au crystals in a "kinetically controlled" pathway [3]. In the present case of amino acids serving as both the reducing agents and capping agents, lower concentrations of amino acids would lower their capping effects, therefore tending to adopt thermodynamically favored and nearly spherical morphologies. Higher concentrations of amino acids, on the other hand, would bring out not only a fast reducing rate but also a low selectivity in {1 1 1} capping (due to chemisorption saturation on all Au facets), thus hindering the formation and growth of 2D Au crystals (Fig. S3). Appropriate concentrations of amino acids, however, would help 2D growth of 2DAC by reorganization or reconnection of Au nanocrystals (Fig. S4a and b).

Further cross-comparison demonstrates that these amino acids have different optimal concentrations to direct 2D growth of Au crystals (see Figs. S1 and S2), and different sizes of 2DAC were obtained by altering amino acids under the same experimental conditions (Fig. 3b). For example, Au microflakes with the lateral dimension over 100 μm were produced with 2.0 mM L-tryptophan, 1.0 mM L-glutamic acid and 1.0 mM L-arginine (Fig. 2). In particular, an impressive lateral size up to 150 μm was achieved by L-tryptophan, and 240 μm by L-arginine, one order of magnitude larger than those in the literature [4] and comparable with Au microflakes synthesized by protein assemblies [5]. The thickness up to 2.4 μm in Figs. 2c and S4c, to the best of our knowledge, is also the largest among 2D Au crystals ever synthesized [3].

The remarkable ability of L-tryptophan, L-glutamic acid and L-arginine in directing 2D growth of large Au microflakes may originate in their appropriate combination of the reducing and capping effects. The reaction rates of amino acids in reducing $HAuCl_4$ were revealed by the variation of a typical Uv–vis absorbance of tetrachloroaurate at 311 nm in Fig. 4, as L-tryptophan < L-glutamic acid and L-aspartic acid < L-arginine < L-lysine. Except L-arginine, this sequence is also in accord with the decreasing lateral size of 2D Au crystals shown in Fig. 3b, e.g. a maximum dimension of 55 μm with L-lysine in sharp contrast to 165 μm with L-tryptophan. It seems that the guanidino group of L-arginine offers a strong chemisorption selectivity to {1 1 1} Au facets, therefore enabling the formation of large Au microflakes.

2DAC spatially scaled within 10^2–10^5 nm were synthesized simply by altering side groups of amino acids in a green bio-mimetic approach, which were immediately invoked to construct diverse functional Au materials or devices. For example, by

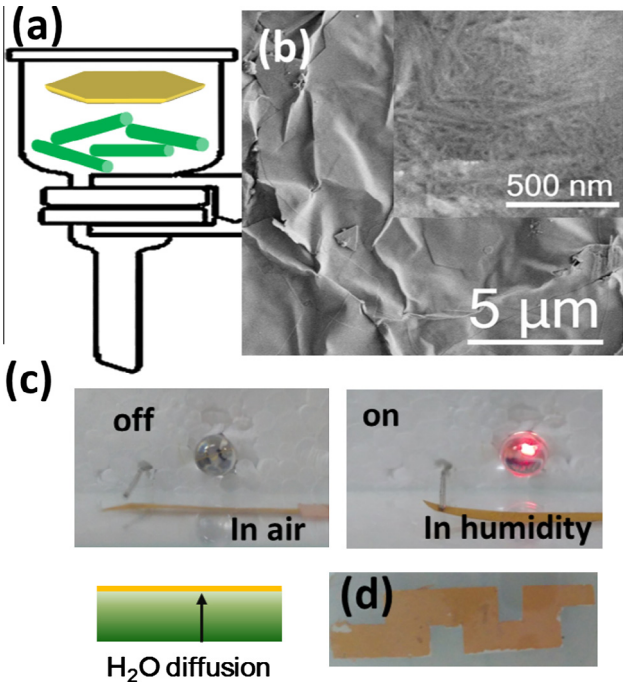

Fig. 5. (a) Schematic representation of sequentially filtering chitin nanofibrils and 2D Au crystals. (b) SEM image of top Au surface of chitin-Au film. The bottom chitin surface was given as the inset. (c) Humidity controlling electric switch constructed with chitin-Au bilayer films. Unsymmetrically swelling in two layers with water in humid air induces the film curl and LED on. (d) Patterning Au layer on chitin nanofibril film.

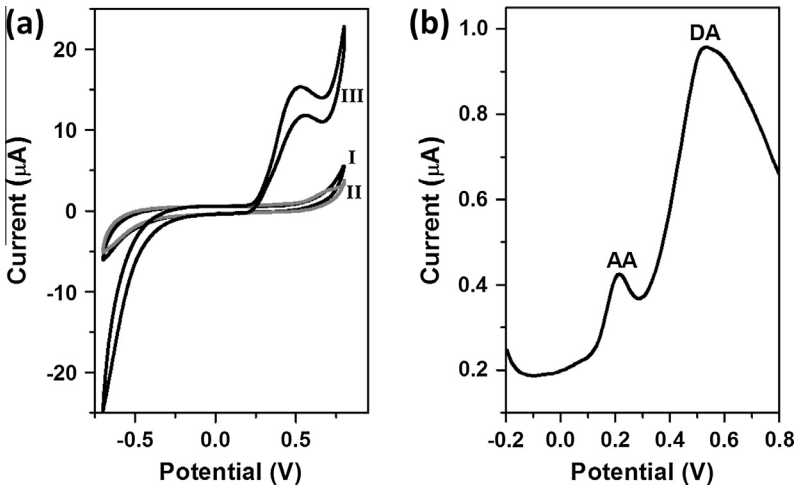

Fig. 6. (a) CV of the electrodes of bare GCE (curve I) and 2DAC-modified GCE (curve III) in the presence of 2 mM H_2O_2. 2DAC modified GCE without H_2O_2 was also measured as the control (curve II). (b) DPSV of 2DAC-modified GCE in the presence of 1.0 mM AA and 0.05 mM DA. 2DAC was synthesized with 1 mM L-arginine.

sequentially filtering the solutions containing chitin nanofibrils extracted from marine crab shells [22] and 2DAC (Fig. S5), bilayer films (thickness ~20 μm) could be produced for multiple applications (see Fig. 5). 2DAC formed a continuous top layer (thickness ~4 μm) with a metallic conductivity of 1.0×10^2 S/cm. The bottom layer of chitin nanofibrils served as a biomass-based substrate [23], meeting the requirements of soft electronics substrates in biological devices, e.g. flexibility, high mechanical property, biocompatibility and biodegradability [24]. Due to higher capability of the chitin layer in absorption and penetration of water than the 2DAC layer, the film showed a reversible shape-memory effect upon cyclic exposure to humidity, making them a promising candidate for humidity sensors and humidity-driving actuators. Accordingly, a humidity-controlling electric switch was constructed to light LED (Fig. 5c). Furthermore, 2DAC layers filtered on commercial filtration membranes could be patterned to specific shapes and transferred on other substrates (e.g. films of chitin nanofibrils, Fig. 5d), potentially serving as electric circuits in diverse electronic devices.

In analogue to Au crystals synthesized before [25], these 2DAC also have high electrochemical catalytic activities and could be used in biosensors. An electrochemical sensor to H_2O_2 was first exampled not only due to its fast-detection, low cost, high sensitivity and good selectivity, but also due to its close association with glucose detection for diabetes mellitus [25]. 2DAC synthesized by 1.0 mM L-arginine was particularly evaluated by immobilizing on GCEs (i.e. 2DAC modified GCE), though showing no significant difference with 2DAC produced by L-lysine (Fig. S6). As shown in Fig. 6a, 2DAC modified GCE exhibited notable redox currents of H_2O_2 (2.0 mM), in contrast to weak electrochemical response of bare GCE. Besides H_2O_2, other molecules of importance for physiological functions of organisms [26] could also be detected by this 2DAC modified GCE, e.g. AA and DA shown in Fig. 6b.

4. Conclusions

In this work, the effect of side groups of amino acids on morphology control of Au crystals was systematically investigated for the first time. Due to the different reducing and/or capping abilities, side group species of amino acids determined not only thickness but also the lateral size of Au crystals. For instance, L-tryptophan (indole group), L-glutamic acid (carboxyethyl group) and L-arginine (guanidino group) were capable of directing 2D growth of Au crystals to synthesize Au microflakes, while only Au nanosheets were synthesized by L-aspartic acid (carboxymethyl group) and L-lysine (amine group). Moreover, by precisely tuning the experimental conditions, 2DAC with lateral size up to 240 μm could be synthesized via L-arginine, much larger than those reported in literatures [4,5,12,13]. When depositing on chitin nanofibrils, the 2DAC could be used for conductive circuits and humidity-responsive actuators, and their catalytic feature further enables them applicable in biosensors. Further studies should focus on exploring the 2DAC with large lateral size (i.e. accessible to the human eye resolution) in bridging nanotechnology and macroscopic device fabrications.

Acknowledgements

National Key Technology R&D Program of Chinese Ministry of Science and Technology (No. 2015BAD14B06), National Natural Science Foundation of China (No. 21474125), Shandong Collaborative Innovation Center for marine biomass fiber materials and textiles and Chinese "1000 youth Talent Program" are kindly acknowledged for financial support.

Appendix A. Supplementary material

SEM images and statistics of Au flakes, Schematic illustration of the dependence of capping effect and reducing effect of amino acids on their concentrations, TEM of chitin nanofibrils, Optical image of chitin-Au bilayer film and cyclic voltammograms. Supplementary data associated with this article can be found, in the online version, at http://dx.doi.org/10.1016/j.jcis.2016.01.004.

References

[1] Y. Xia, Y. Xiong, B. Lim, S.E. Skrabalak, Shape-controlled synthesis of metal nanocrystals: simple chemistry meets complex physics?, Angew Chem. Int. Ed. 48 (2009) 60–103, http://dx.doi.org/10.1002/anie.200802248.
[2] N. Li, P. Zhao, D. Astruc, Anisotropic gold nanoparticles: synthesis, properties, applications, and toxicity, Angew. Chem. Int. Ed. 53 (2014) 1756–1789, http://dx.doi.org/10.1002/anie.201300441.
[3] H. Hu, J. Zhou, Q. Kong, C. Li, Two-dimensional Au nanocrystals: shape/size controlling synthesis, morphologies, and applications, Part. Part. Syst. Charact. 32 (2015) 796–808, http://dx.doi.org/10.1002/ppsc.201500035.
[4] G.D. Moon, G.-H. Lim, J.H. Song, M. Shin, T. Yu, B. Lim, et al., Highly stretchable patterned gold electrodes made of Au nanosheets, Adv. Mater. 25 (2013) 2707–2712, http://dx.doi.org/10.1002/adma.201300794.
[5] J. Zhou, A. Saha, J. Adamcik, H. Hu, Q. Kong, C. Li, et al., Macroscopic single-crystal gold microflakes and their devices, Adv. Mater. 27 (2015) 1945–1950, http://dx.doi.org/10.1002/adma.201405121.

[6] N. Liu, M.L. Tang, M. Hentschel, H. Giessen, A.P. Alivisatos, Nanoantenna-enhanced gas sensing in a single tailored nanofocus, Nat. Mater. 10 (2011) 631–636, http://dx.doi.org/10.1038/nmat3029.
[7] C. Lofton, W. Sigmund, Mechanisms controlling crystal habits of gold and silver colloids, Adv. Funct. Mater. 15 (2005) 1197–1208, http://dx.doi.org/10.1002/adfm.200400091.
[8] K. Banu, T. Shimura, Synthesis of large-scale transparent gold nanosheets sandwiched between stabilizers at a solid–liquid interface, New J. Chem. 36 (2012) 2112–2120, http://dx.doi.org/10.1039/C2NJ40478H.
[9] T. Kida, Synthesis of gold nanosheets at a liquid/liquid interface using an amphiphilic polyoxometallate/surfactant hybrid photocatalyst, Langmuir 24 (2008) 7648–7650, http://dx.doi.org/10.1021/la801804w.
[10] H.L. Qin, D. Wang, Z.L. Huang, D.M. Wu, Z.C. Zeng, B. Ren, et al., Thickness-controlled synthesis of ultrathin Au sheets and surface plasmonic property, J. Am. Chem. Soc. 135 (2013) 12544–12547, http://dx.doi.org/10.1021/ja406107u.
[11] S.-H. Cha, J.-U. Kim, K.-H. Kim, J.-C. Lee, Preparation of gold nanosheets using poly(ethylene oxide)–poly(propylene oxide)–poly(ethylene oxide) block copolymers via photoreduction, Mater. Sci. Eng. B 140 (2007) 182–186, http://dx.doi.org/10.1016/j.mseb.2007.03.016.
[12] W.J. Crookes-Goodson, J.M. Slocik, R.R. Naik, Bio-directed synthesis and assembly of nanomaterials, Chem. Soc. Rev. 37 (2008) 2403–2412, http://dx.doi.org/10.1039/B702825N.
[13] C. Li, S. Bolisetty, R. Mezzenga, Hybrid nanocomposites of gold single-crystal platelets and amyloid fibrils with tunable fluorescence, conductivity, and sensing properties, Adv. Mater. 25 (2013) 3694–3700, http://dx.doi.org/10.1002/adma.201300904.
[14] D. Wei, W. Qian, Y. Shi, S. Ding, Y. Xia, Mass synthesis of single-crystal gold nanosheets based on chitosan, Carbohydr. Res. 342 (2007) 2494–2499, http://dx.doi.org/10.1016/j.carres.2007.07.001.
[15] L. Wang, C.-H. Liu, Y. Nemoto, N. Fukata, K.C.-W. Wu, Y. Yamauchi, Rapid synthesis of biocompatible gold nanoflowers with tailored surface textures with the assistance of amino acid molecules, RSC Adv. 2 (2012) 4608, http://dx.doi.org/10.1039/c2ra20348k.
[16] S.K. Srivastava, T. Hasegawa, R. Yamada, C. Ogino, M. Mizuhata, A. Kondo, Green synthesis of Au, Pd and Au@Pd core–shell nanoparticles via a tryptophan induced supramolecular interface, RSC Adv. 3 (2013) 18367–18372, http://dx.doi.org/10.1039/C3RA43389G.
[17] M. Kasture, M. Sastry, B.L.V. Prasad, Halide ion controlled shape dependent gold nanoparticle synthesis with tryptophan as reducing agent: enhanced fluorescent properties and white light emission, Chem. Phys. Lett. 484 (2010) 271–275, http://dx.doi.org/10.1016/j.cplett.2009.11.052.
[18] Y. Shao, Y. Jin, S. Dong, Synthesis of gold nanoplates by aspartate reduction of gold chloride, Chem. Commun. (2004) 1104–1105, http://dx.doi.org/10.1039/B315732F.
[19] M. Iosin, P. Baldeck, S. Astilean, Study of tryptophan assisted synthesis of gold nanoparticles by combining UV–Vis, fluorescence, and SERS spectroscopy, J. Nanoparticle Res. 12 (2010) 2843–2849, http://dx.doi.org/10.1007/s11051-010-9869-6.
[20] Y.N. Tan, J.Y. Lee, D.I.C. Wang, Aspartic acid synthesis of crystalline gold nanoplates, nanoribbons, and nanowires in aqueous solutions, J. Phys. Chem. C. 112 (2008) 5463–5470, http://dx.doi.org/10.1021/jp800501k.
[21] T. Maruyama, Y. Fujimoto, T. Maekawa, Synthesis of gold nanoparticles using various amino acids, J. Colloid Interface Sci. 447 (2015) 254–257, http://dx.doi.org/10.1016/j.jcis.2014.12.046.
[22] S. Ifuku, M. Nogi, K. Abe, M. Yoshioka, M. Morimoto, H. Saimoto, et al., Preparation of chitin nanofibers with a uniform width as α-chitin from crab shells, Biomacromolecules 10 (2009) 1584–1588, http://dx.doi.org/10.1021/bm900163d.
[23] J. Wu, J.C. Meredith, Assembly of chitin nanofibers into porous biomimetic structures via freeze drying, ACS Macro Lett. 3 (2014) 185–190, http://dx.doi.org/10.1021/mz400543f.
[24] M.A. Daniele, A.J. Knight, S.A. Roberts, K. Radom, J.S. Erickson, Sweet substrate: a polysaccharide nanocomposite for conformal electronic decals, Adv. Mater. 27 (2015) 1600–1606, http://dx.doi.org/10.1002/adma.201404445.
[25] Y. Zhang, G. Chang, S. Liu, W. Lu, J. Tian, X. Sun, A new preparation of Au nanoplates and their application for glucose sensing, Biosens. Bioelectron. 28 (2011) 344–348, http://dx.doi.org/10.1016/j.bios.2011.07.041.
[26] Z.-H. Sheng, X.-Q. Zheng, J.-Y. Xu, W.-J. Bao, F.-B. Wang, X.-H. Xia, Electrochemical sensor based on nitrogen doped graphene: simultaneous determination of ascorbic acid, dopamine and uric acid, Biosens. Bioelectron. 34 (2012) 125–131, http://dx.doi.org/10.1016/j.bios.2012.01.030.